Process water recovery via forward osmosis: membrane and integrated process development

J. Martin, G. Kolliopoulos and V. G. Papangelakis

ABSTRACT

This work reports on efforts to develop an integrated continuous forward osmosis system for the recovery of water from wastewater streams, highlighting critical process parameters to minimize energy consumption. Forward osmosis experiments were performed using NaCl draw solutions of various concentrations and the intrinsic membrane parameters (water permeability, draw solution permeability, and structural parameter) were then determined via nonlinear regression using MATLAB. The experimental data were then used to validate a theoretical water flux model, which was subsequently applied to simulate the forward osmosis performance under different hydrodynamic conditions using both NaCl and TMA-CO_2-H_2O (TMA: trimethylamine) draw solutions. Analysis of the energy efficiency of the TMA-CO_2 draw solution regeneration stage revealed that the draw solution flow rate has a significant impact on energy consumption. Also, increasing the feed flow rate was found to slightly enhance the water flux up to 2.5%, while having a negligible impact on the downstream regeneration process energy consumption.

Key words | process optimization, sustainability, wastewater recovery, water conservation

J. Martin
G. Kolliopoulos
V. G. Papangelakis (corresponding author)
University of Toronto,
200 College St., Toronto, ON M5S 3H7,
Canada
E-mail: *vladimiros.papangelakis@utoronto.ca*

HIGHLIGHTS

- Simulated effects of hydrodynamic conditions on forward osmosis membrane performance are investigated for NaCl and trimethylamine-CO_2 draw solutes.
- Increased mass transfer is observed with increased feed and draw solution flow rates.
- Increased draw solution flow rate significantly increases the thermal draw solution regeneration process energy consumption.
- Negligible changes to draw solution regeneration energy consumption were found with increasing feed flow rate.

doi: 10.2166/wst.2020.256

GRAPHICAL ABSTRACT

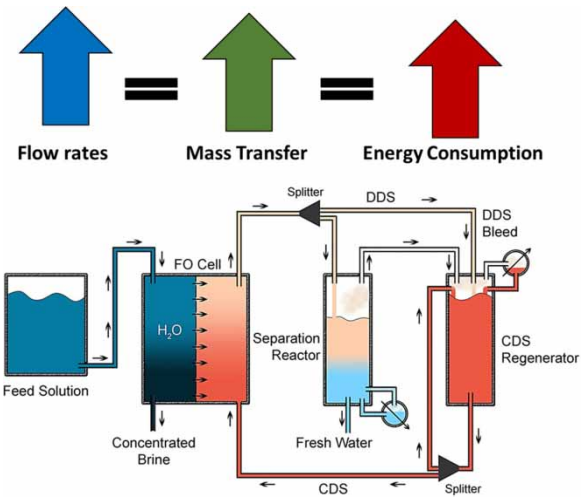

INTRODUCTION

Industrial wastewater treatment poses a substantial economic and environmental challenge, for it is necessary to recover clean water for reuse while reducing the volume of the effluent. Current pressure-driven water recovery processes like reverse osmosis are limited by the maximum concentration of water that can be economically processed due to the fouling propensity (Lee *et al.* 2010). Additionally, thermal processes like distillation or crystallization/evaporation have high energy consumption and operating expenditures (Kolliopoulos & Papangelakis 2018). Compared to traditional water recovery technology, forward osmosis (FO) is an attractive solution due to its low fouling potential (Lee *et al.* 2010) and favourable energy consumption (Kolliopoulos Martin & Papangelakis 2018).

Driven by an osmotic pressure differential, FO uses a concentrated draw solution (CDS) to spontaneously pull water across a semipermeable membrane from an effluent, rejecting and concentrating effluent solutes across the membrane. Although the FO process occurs spontaneously, energy is required to recover water from the diluted draw solution (DDS) and regenerate the CDS. This draw solution regeneration stage is dependent on the type of draw solution used including: reverse osmosis for inorganic salts (Martinetti Childress & Cath 2009; Altaee *et al.* 2014), magnetic-driven separation for magnetic nanoparticles (Ling Wang & Chung 2010), and thermal-driven separation for thermolytic draw solutions (Kolliopoulos Martin & Papangelakis 2018). To date there has been extensive analysis of the FO membrane stage, but as FO approaches industrial-scale adoption, the focus shifts to the overall integrated FO process, of both the membrane and draw solution regeneration stages.

The impact of hydrodynamic conditions on FO performance has been analysed in previous studies (Tan & Ng 2008; Hancock & Cath 2009; Jung *et al.* 2011; Phuntsho *et al.* 2014; Bui Arena & McCutcheon 2015; Tow *et al.* 2015); however, little attention has been given to the interaction effects between the feed and draw solution flow rates. Additionally, there lacks sufficient analysis of how changes to the flow rates in the membrane stage affect the downstream draw solution regeneration process, particularly for the thermolytic draw solution TMA-CO_2-H_2O (TMA: trimethylamine). Through an experimentally verified model, this research investigates the simulated effects of hydrodynamic conditions in the membrane stage on the energy consumption of the overall integrated FO process (membrane and draw solution regeneration stages). The thermal regeneration of the TMA-CO_2-H_2O draw solution is determined using the process outlined in Kolliopoulos Martin & Papangelakis (2018). The dependence of the water and reverse draw solution flux on the feed and the draw solution flow rates in the FO membrane stage are also examined through simulation using both the NaCl and TMA-CO_2-H_2O draw solutions.

MATERIALS AND METHODS

A list of the materials used, their source, and their assay as specified by the supplier is presented in Table 1.

Table 1 | Materials

Chemical name	CAS no.	Source	Purity-assay[a]
NaCl Certified ACS Crystalline	7647-14-5	Fisher Sci.	99.6%
DI water	7732-18-5	Milli Q Ref. Serial No. F2AA58473D	18.2 MΩ·cm

[a]As stated by the supplier.

The FO apparatus schematic is illustrated in Figure 1, featuring a rectangular stainless steel CF042-FO cell, obtained from Sterlitech (active area of 42 cm^2) and an asymmetric cellulose triacetate membrane, obtained from Fluid Technology Solutions. The membrane was oriented with the active layer facing the feed side. The FO cell was run counter-currently, and the flow rates were controlled by a Thermo-Fisher Easy Load II peristaltic pump.

For the model-validation experiments, 0.5, 1, 2, and 3.5 M NaCl solutions were used as the CDS and deionized (DI) water used as the feed solution. NaCl was used for the model validation as it is a widely studied draw solute, with comparable FO performance to that of TMA-CO_2-H_2O (Boo Khalil & Elimelech 2015) and is suitable for establishing a baseline for FO performance. The draw solutions were prepared by dissolving the appropriate amount of the draw solute also in DI water. The draw and feed solutions were recirculated in individual closed loops, with two solution reservoirs of a large enough volume (2 L) to ensure an approximately constant concentration. A mass flow rate of 8,000 g/h was used for both streams. Every 30 sec the mass of each reservoir was recorded digitally by Mettler-Toledo balances. Both draw and feed solution samples were taken at steady state (within 15 min), and again at the conclusion of the experiment (1 h). From these samples both the feed and draw solution cation concentrations were determined using inductively coupled plasma optical emission spectrometry (Agilent 700 series ICP-OES). Prior to analysis, the samples were diluted with 5% nitric acid: 50× for the feed samples, and 1,000× for the draw solution samples. The water flux was determined based on the draw solution mass change, while the reverse draw solute flux was determined based on the change in the solute concentration in the feed.

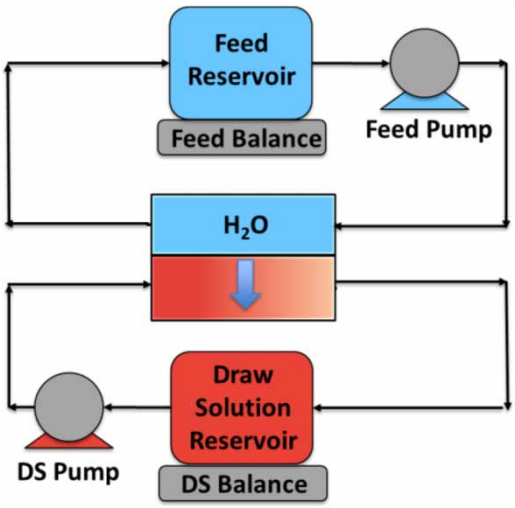

Figure 1 | Forward osmosis experimental apparatus.

For the flow rate analysis, using the verified model, the draw solution and feed stream mass flow rates were varied between 250 and 2,000 g/h to reflect those suitable for the laboratory-scale draw solution regeneration stage described in (Kolliopoulos Martin & Papangelakis 2018). The simulations also assumed a draw solution concentration of 3 M and a feed of 0.5 M NaCl. The energy consumption to regenerate a 3 M TMA-CO_2-H_2O draw solution via a thermal stripping and adsorption column apparatus, was estimated using OLI Flowsheet software (Kolliopoulos Martin & Papangelakis 2018) with the resulting DDS composition and flow rate simulated using Equation (1) as input conditions.

To model the water flux, J_w (L/(m^2·h)), for the FO membrane stage the following equation is used (Bui Arena & McCutcheon 2015):

$$J_W = A\left\{\frac{\pi_{D,b}\exp\left[-J_w\left(\frac{1}{k_D}+\frac{S}{D_D}\right)\right]-\pi_{F,b}\exp\left(\frac{J_w}{k_F}\right)}{1+\frac{B}{J_w}\left\{\exp\left(\frac{J_w}{k_F}\right)-\exp\left[-J_w\left(\frac{1}{k_D}+\frac{S}{D_D}\right)\right]\right\}}\right\} \quad (1)$$

where A (L/(m^2·h·bar)) denotes the water permeability coefficient of the membrane, B denotes the draw solute permeability coefficient of the membrane (L/(m^2·h)), π is the osmotic pressure of the draw solution and feed respectively (bar), S is the structural parameter of the membrane (m), D is the draw solute diffusion coefficient (m^2/s), and k is the mass transfer coefficient of the draw solute in the feed or draw solution respectively (m/s), respectively. The subscripts D, F, and b refer to the draw solution, the feed side of the membrane, and the bulk solutions, respectively.

Concentration polarization is a localized concentration gradient that occurs at membrane–solution interfaces due to the selective transport of water across the membrane, rejecting and accumulating solutes at the membrane–solution

interface. In FO, concentration polarization occurs within the porous membrane support (internal) and at the membrane and solution interfaces (external).

Equation (1) considers internal concentration polarization, draw and feed side external concentration polarization, and the reverse flux of the draw solute. It is critical to consider all forms of concentration polarization as increases in both the draw solution and feed stream flow rates result in increased water flux due to decreased external concentration polarization (Tan & Ng 2008; Phuntsho *et al.* 2014), and the draw solution flow rate affects the transport of water into the porous support structure, reducing internal concentration polarization (Beavers & Joseph 1967; Bui Arena & McCutcheon 2015).

The reverse salt flux, J_s (mol/(m^2·h)), is similarly calculated using Equation (2):

$$J_s = B\left\{\frac{C_{D,b}\exp\left[-J_w\left(\frac{1}{k_D}+\frac{S}{D_D}\right)\right]-C_{F,b}\exp\left(\frac{J_w}{k_F}\right)}{1+\frac{B}{J_w}\left\{\exp\left(\frac{J_w}{k_F}\right)-\exp\left[-J_w\left(\frac{1}{k_D}+\frac{S}{D_D}\right)\right]\right\}}\right\} \quad (2)$$

The intrinsic membrane parameters used in Equations (1) and (2), A, B, and S, for NaCl in our system were obtained through non-linear regression using MATLAB software (Tiraferri *et al.* 2013), and they are presented in Table 2. The permeability of the TMA-CO_2-H_2O draw solution B was obtained from Boo Khalil & Elimelech (2015) and used with the water permeability and structural parameter regressed from the experimental NaCl data in this work.

The osmotic pressure was determined using the OLI Stream Analyzer Version 9.6 software with the MSE (mixed solvent electrolyte) model. The diffusion coefficient of the cation and anion for each draw solute species, D_1 and D_2, were also obtained from OLI software and then used to obtain the average draw solute diffusion coefficient, D (Ghiu Carnahan & Barger 2002).

The mass transfer coefficient k_i of the draw solute in stream i, is obtained from the following correlation (Phuntsho *et al.* 2014):

$$k_i = \frac{Sh_i D_i}{d_h} \quad (3)$$

where Sh refers to the Sherwood number and d_h the hydraulic diameter of the respective channel through which the fluid is flowing (m). The Sherwood number is obtained from the following for laminar flow:

$$Sh_i = 1.85\left(Re_i Sc_i \frac{d_h}{L_i}\right)^{0.33} \quad (4)$$

where Re is the Reynolds number, Sc is the Schmidt number, and L is the characteristic length of the respective channel (m). The Reynolds number is determined using the following equation:

$$Re_i = \frac{\rho_i v_i d_h}{\mu_i} \quad (5)$$

where μ represents the dynamic viscosity (kg/(m·s)), ρ the density (kg/m^3), and v the velocity (m/s) of the solution respectively. Additionally, the Schmidt number is calculated using Equation (6):

$$Sc_i = \frac{\mu_i}{\rho_i D_i} \quad (6)$$

The solution density and its kinematic viscosity were determined using the OLI Studio software with the MSE model.

Table 2 | Intrinsic membrane parameters used for modelling

Draw solution species	Water permeability, A (L/(m^2·h·bar))	Draw solution permeability, B (L/(m^2·h))	Structural parameter, S (μm)
NaCl	0.349	0.451	573
TMA-CO_2-H_2O	…	0.31	…

RESULTS AND DISCUSSION

The experimental water flux and reverse draw solution flux for concentrations of 0.5–3.5 M NaCl draw solutions were compared to the model results. Although diverging from experimental results by up to 50% at low draw solution concentrations (absolute difference of 3.6 L/(m^2·h)), Equation (1) displays reasonable agreement with the water flux measurements (Figure 2) particularly at high draw solution concentration values. In contrast, Equation (2) displays poor agreement with the reverse draw solution flux measurements (Figure 3), particularly at higher draw solution concentrations. This deviation from our experimental results is due to certain model assumptions, including that of Van't Hoff's law validity at high draw

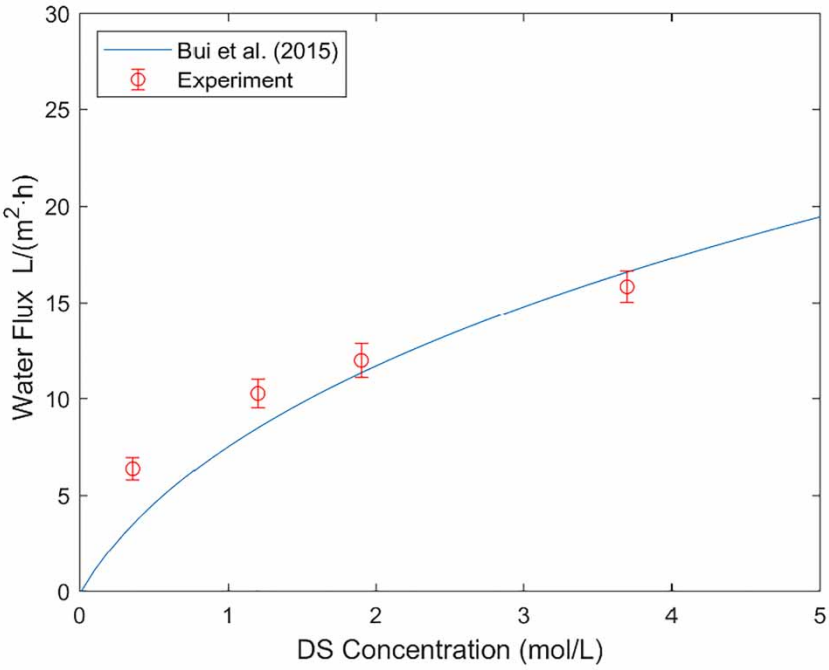

Figure 2 | Water flux model experimental validation.

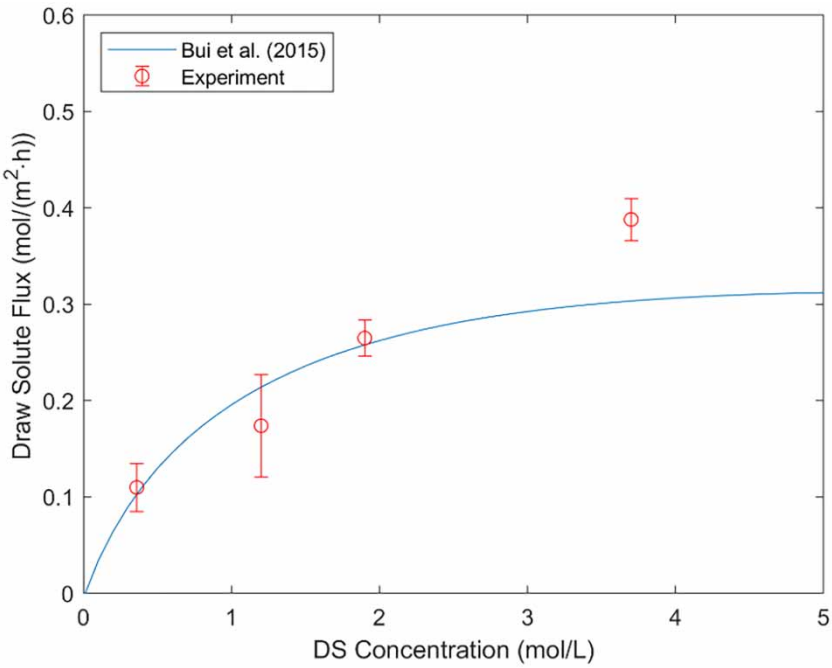

Figure 3 | Reverse draw solute flux model experimental validation.

solution concentrations and that of constant draw solution physical properties. However, the overall fit of the model equations is deemed suitable for the subsequent calculations.

The impact of the feed and draw solution flow rates on the water and reverse draw solution flux were simulated using the aforementioned mass transfer model using both 3 M NaCl and 3 M TMA-CO_2-H_2O draw solutions with a

0.5 M NaCl feed. The results for the NaCl draw solution in Figure 4 display an increase in the water flux of up to 5.7% by increasing both the feed and draw solution flow rates under these conditions; however, the feed flow rate was observed to have a lower impact on the water flux. This is due to the reduction in external concentration polarization on both sides of the membrane, reducing the inhibition for mass transport across the membrane.

Similarly, the reverse draw solution flux depends on both the feed and draw solution flow rates (Figure 5), suggesting that both forms of external concentration polarization have an impact on the transfer of the draw solute across the membrane. Therefore, increasing the feed mass flow rate enhances the water flux but at the cost of greater draw solution losses, while increasing the draw solution flow rate will further maximize the water flux with a less significant increase in the reverse draw solution flux. It is likely that the feed flow rate will have a more significant impact on the FO performance for more concentrated feed solutions, as the resistance to mass transfer will increase.

Additional simulations using a 3 M TMA-CO_2-H_2O draw solution (Figures 6 and 7) with a 0.5 M NaCl feed indicate similar results to those using the NaCl draw solution. Increases to both the feed and draw solution flow rates will increase the mass transfer of all species across the membrane, thus increasing both the water flux and reverse draw solute flux (up to 5.7% and 9.4% respectively). Further, the draw solution flow rate has a greater impact on the water flux than that of the feed flow rate for both the inorganic and organic draw solution examined.

To illustrate how process parameters in the membrane stage can affect the integrated FO process, the energy consumption (kWh/m^3 of fresh water produced) of the lab-scale thermal draw solution regeneration process for TMA-CO_2-H_2O, outlined in Kolliopoulos Martin & Papangelakis (2018), was determined using various feed and draw solution flow rates (Figure 8). It is obvious that increased feed and draw solution flow rates will increase both the transport of the draw solute and water across the membrane, resulting in an increased energy demand to regenerate the draw solution. These concentration changes were taken into account.

Energy consumption is maximized at high draw solution flow rates and plateaus at a draw solution flow rate of 1,500 g/h. These results indicate that process flow rate optimization is essential in the FO process operation, as the energy consumption can decrease by 15% by adjusting the draw solution flow rate. Interestingly, increases in the feed mass flow rate have a negligible effect on the downstream process energy consumption, while providing an enhanced water flux. This further suggests that the energy consumption for the downstream regeneration process is highly dependent on the draw solution flow rate and less so on the water flux across the membrane when they differ by two orders of magnitude. Therefore, process changes that enhance the water flux across the membrane, such as

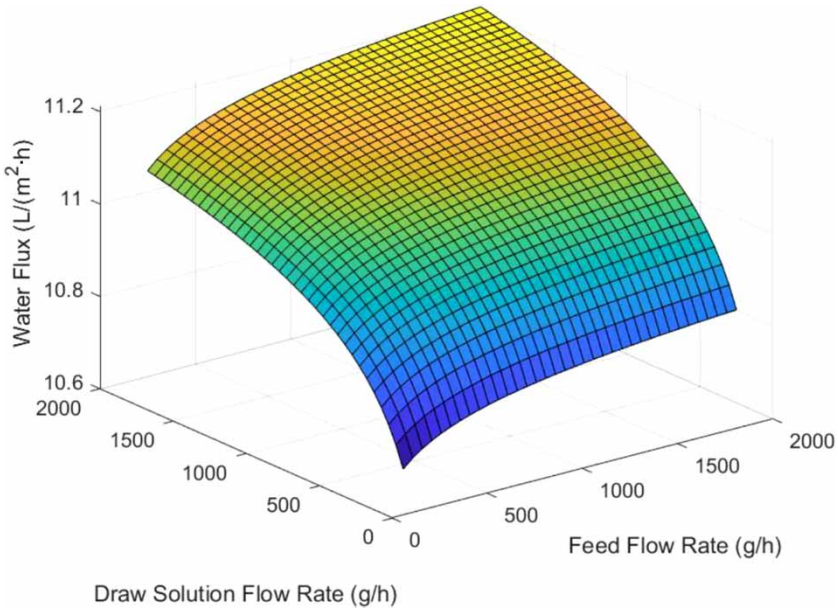

Figure 4 | Water flux dependence on draw solution (3 M NaCl) and feed (0.5 M NaCl) flow rates.

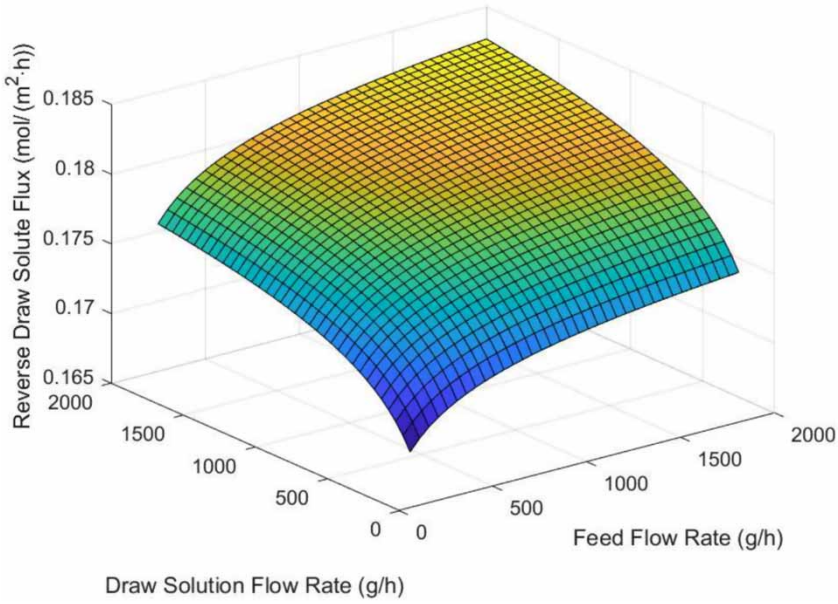

Figure 5 | Reverse draw solution flux dependence on draw solution (3 M NaCl) and feed (0.5 M NaCl) flow rates.

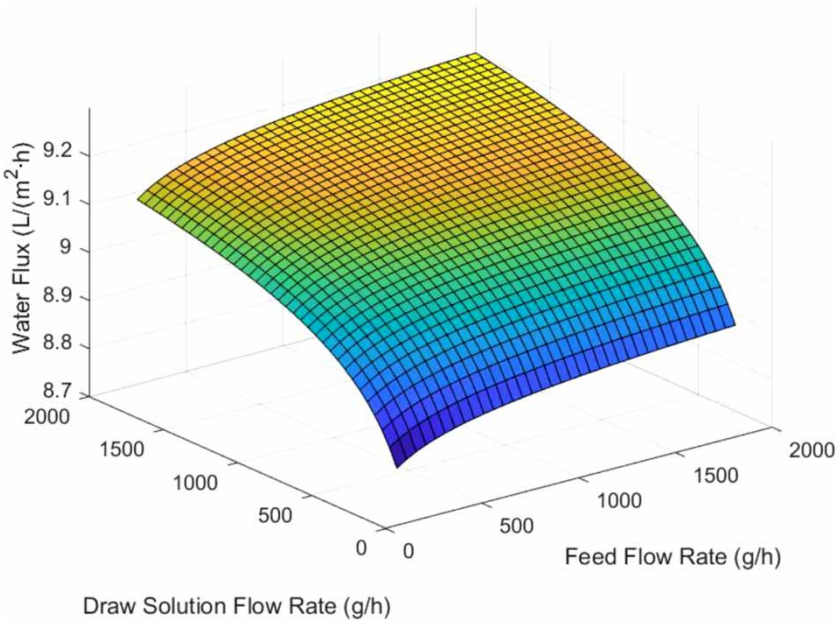

Figure 6 | Water flux dependence on draw solution (3 M TMA-CO_2-H_2O) and feed (0.5 M NaCl) flow rates.

membrane orientation, will have minor impact to the energy consumption for the regeneration process.

CONCLUSIONS

As predicted, both the feed and the draw solution flow rates affect the FO performance for both inorganic and organic draw solutes with different physical properties. Both the water flux and reverse draw solution flux increase with increasing draw solution flow rate. However, the feed solution flow rate has less impact on the water flux. Therefore, increasing the feed flow rate can be used to enhance the water flux by 5.7% with a negligible impact on the downstream thermal regeneration process energy consumption, but the reverse draw solution flux will increase by 10%.

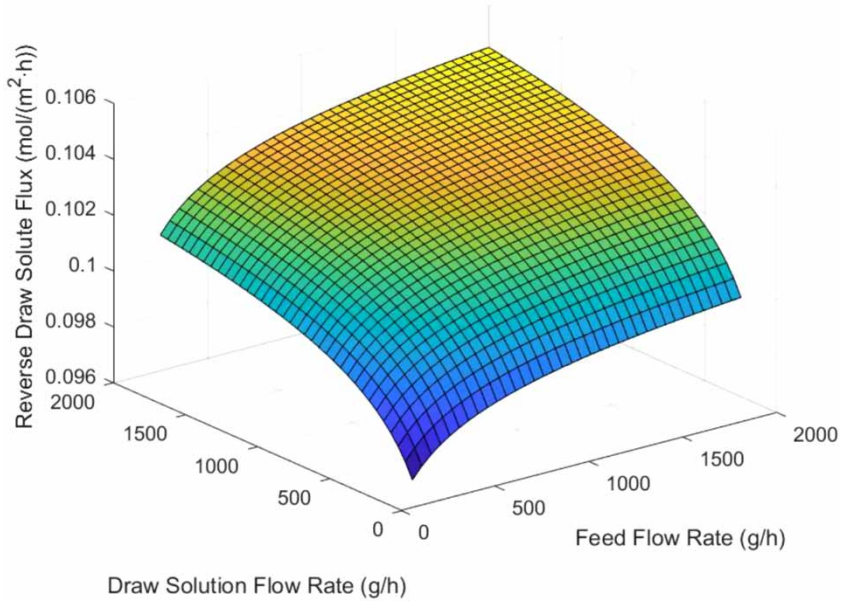

Figure 7 | Reverse draw solute flux dependence on draw solution (3 M TMA-CO_2-H_2O) and feed (0.5 M NaCl) flow rates.

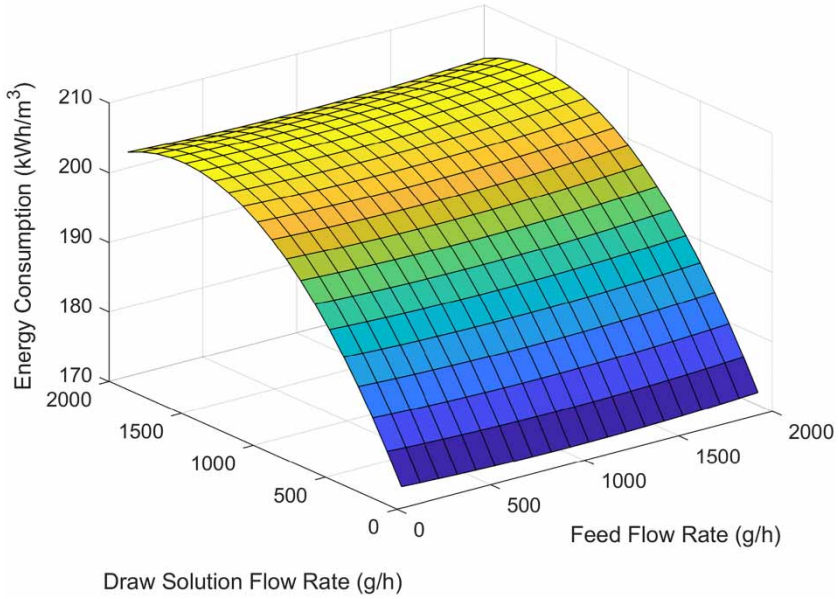

Figure 8 | Energy consumption dependence of the integrated FO process on the draw solution and feed flow rates in the membrane stage.

Further analysis is required to determine the flow rate effects for alternative draw solution regeneration processes (e.g., reverse osmosis, coagulation) as well as for feed streams that contain dissolved solids with additional polarization events. Additional cost analysis is also recommended for multiple draw solution regeneration applications and optimization studies are recommended on a case-by-case basis for all FO applications.

ACKNOWLEDGEMENTS

The authors acknowledge gratefully the Natural Sciences and Engineering Research Council of Canada (NSERC RPGIN 105655-2013), and the University of Toronto Connaught Innovation Fund (Fund #506081) for providing financial support. OLI Systems Inc. is also acknowledged for providing access to the software.

REFERENCES

Altaee, A., Zaragoza, G. & Rost van Tonningen, H. 2014 Comparison between forward osmosis-reverse osmosis and reverse osmosis processes for seawater desalination. *Desalination* **336** (1), 50–57. https://doi.org/10.1016/j.desal.2014.01.002.

Beavers, G. S. & Joseph, D. D. 1967 Boundary conditions at a naturally permeable wall. *Journal of Fluid Mechanics*. https://doi.org/10.1017/S0022112067001375.

Boo, C., Khalil, Y. F. & Elimelech, M. 2015 Performance evaluation of trimethylamine-carbon dioxide thermolytic draw solution for engineered osmosis. *Journal of Membrane Science* **473**, 302–309. https://doi.org/10.1016/j.memsci.2014.09.026.

Bui, N. N., Arena, J. T. & McCutcheon, J. R. 2015 Proper accounting of mass transfer resistances in forward osmosis: improving the accuracy of model predictions of structural parameter. *Journal of Membrane Science* **492**, 289–302. https://doi.org/10.1016/j.memsci.2015.02.001.

Ghiu, S. S., Carnahan, R. & Barger, M. 2002 Permeability of electrolytes through a flat RO membrane in a direct osmosis study. *Desalination*. https://doi.org/10.1016/S0011-9164(02)00348-X.

Hancock, N. T. & Cath, T. Y. 2009 Solute coupled diffusion in osmotically driven membrane processes. *Environmental Science and Technology*. https://doi.org/10.1021/es901132x.

Jung, D. H., Lee, J., Kim, D. Y., Lee, Y. G., Park, M., Lee, S., Yang, D. R. & Kim, J. H. 2011 Simulation of forward osmosis membrane process: effect of membrane orientation and flow direction of feed and draw solutions. *Desalination* **277** (1–3), 83–91. https://doi.org/10.1016/j.desal.2011.04.001.

Kolliopoulos, G. & Papangelakis, V. G. 2018 *Extraction 2018*. Springer International Publishing. https://doi.org/10.1007/978-3-319-95022-8.

Kolliopoulos, G., Martin, J. T. & Papangelakis, V. G. 2018 Energy requirements in the separation-regeneration step in forward osmosis using TMA–CO_2–H_2O as the draw solution. *Chemical Engineering Research and Design*. https://doi.org/10.1016/j.cherd.2018.10.015.

Lee, S., Boo, C., Elimelech, M. & Hong, S. 2010 Comparison of fouling behavior in forward osmosis (FO) and reverse osmosis (RO). *Journal of Membrane Science* **365** (1–2), 34–39. https://doi.org/10.1016/j.memsci.2010.08.036.

Ling, M. M., Wang, K. Y. & Chung, T. S. 2010 Highly water-soluble magnetic nanoparticles as novel draw solutes in forward osmosis for water reuse. *Industrial and Engineering Chemistry Research* **49** (12), 5869–5876. https://doi.org/10.1021/ie100438x.

Martinetti, C. R., Childress, A. E. & Cath, T. Y. 2009 High recovery of concentrated RO brines using forward osmosis and membrane distillation. *Journal of Membrane Science*. https://doi.org/10.1016/j.memsci.2009.01.003.

Phuntsho, S., Hong, S., Elimelech, M. & Shon, H. K. 2014 Osmotic equilibrium in the forward osmosis process: modelling, experiments and implications for process performance. *Journal of Membrane Science* **453**, 240–252. https://doi.org/10.1016/j.memsci.2013.11.009.

Tan, C. H. & Ng, H. Y. 2008 Modified models to predict flux behavior in forward osmosis in consideration of external and internal concentration polarizations. *Journal of Membrane Science* **324** (1–2), 209–219. https://doi.org/10.1016/j.memsci.2008.07.020.

Tiraferri, A., Yip, N. Y., Straub, A. P., Castrillon, S. R.-V. & Elimelech, M. 2013 A method for the simultaneous determination of transport and structural parameters of forward osmosis membranes. *Journal of Membrane Science* **444**, 523–538. https://doi.org/10.1016/j.memsci.2013.05.023.

Tow, E. W., McGovern, R. K. & Lienhard V, J. H. 2015 Raising forward osmosis brine concentration efficiency through flow rate optimization. *Desalination*. https://doi.org/10.1016/j.desal.2014.10.034.

First received 6 August 2019; accepted in revised form 15 May 2020. Available online 26 May 2020